Isotropic Three-Dimensional T_2 Mapping of Knee Cartilage: Development and Validation

Roberto Colotti, MSc,[1] Patrick Omoumi, MD, PhD,[1] Gabriele Bonanno, PhD,[1,2,3] Jean-Baptiste Ledoux, BSc,[1,4] and Ruud B. van Heeswijk, PhD[1]*

Purpose: 1) To implement a higher-resolution isotropic 3D T_2 mapping technique that uses sequential T_2-prepared segmented gradient-recalled echo (Iso3DGRE) images for knee cartilage evaluation, and 2) to validate it both in vitro and in vivo in healthy volunteers and patients with knee osteoarthritis.
Materials and Methods: The Iso3DGRE sequence with an isotropic 0.6 mm spatial resolution was developed on a clinical 3T MR scanner. Numerical simulations were performed to optimize the pulse sequence parameters. A phantom study was performed to validate the T_2 estimation accuracy. The repeatability of the sequence was assessed in healthy volunteers (n = 7). T_2 values were compared with those from a clinical standard 2D multislice multiecho (MSME) T_2 mapping sequence in knees of healthy volunteers (n = 13) and in patients with knee osteoarthritis (OA, n = 5).
Results: The numerical simulations resulted in 100 excitations per segment and an optimal radiofrequency (RF) excitation angle of 15°. The phantom study demonstrated a good correlation of the technique with the reference standard (slope 0.9 ± 0.05, intercept 0.2 ± 1.7 msec, $R^2 \geq 0.99$). Repeated measurements of cartilage T_2 values in healthy volunteers showed a coefficient of variation of 5.6%. Both Iso3DGRE and MSME techniques found significantly higher cartilage T_2 values ($P < 0.03$) in OA patients. Iso3DGRE precision was equal to that of the MSME T_2 mapping in healthy volunteers, and significantly higher in OA ($P = 0.01$).
Conclusion: This study successfully demonstrated that high-resolution isotropic 3D T_2 mapping for knee cartilage characterization is feasible, accurate, repeatable, and precise. The technique allows for multiplanar reformatting and thus T_2 quantification in any plane of interest.
Level of Evidence: 1
Technical Efficacy: Stage 2

J. MAGN. RESON. IMAGING 2018;47:362–371.

To date, no effective cure exists to slow down or stop the progression of osteoarthritis (OA), a condition characterized by progressive cartilage degeneration.[1] Because cartilage has limited repair capacity, the early detection of any local damage that precedes permanent cartilage tissue loss is an important target for research. Compositional magnetic resonance imaging (MRI) techniques have the potential to reflect the biochemical and ultrastructural composition of cartilage and provide quantitative information at the early stages of OA.[1–3] Among these compositional MRI sequences, T_2 mapping is used most in the clinic.[1]

The spin-spin or T_2 relaxation time is a physiological tissue property that reflects the water and collagen content of the extracellular matrix, as well as the structure of the collagen network.[1,4] T_2 relaxometry has been validated as a valuable quantitative imaging biomarker of the early changes of cartilage ultrastructure, and as an outcome measure for the development of new therapeutic solutions and cartilage repair procedures.[3,5] In addition, the T_2 relaxation time increases with the severity of OA and it can thus be also exploited for the grading of cartilage degeneration.[6]

View this article online at wileyonlinelibrary.com. DOI: 10.1002/jmri.25755

Received Feb 14, 2017, Accepted for publication Apr 18, 2017.

*Address reprint requests to: R.B.v.H., Department of Radiology, Lausanne University Hospital (CHUV), Rue de Bugnon 46, BH 08.084, 1011 Lausanne, Switzerland. E-mail: ruud.mri@gmail.com

P. Omoumi and R.B. van Heeswijk contributed equally to this work.

From the [1]Department of Radiology, University Hospital (CHUV) and University of Lausanne (UNIL), Lausanne, Switzerland; [2]Division of Cardiology, Department of Medicine, Johns Hopkins University, Baltimore, Maryland, USA; [3]Division of MR Research, Russell Morgan Department of Radiology and Radiological Sciences, Johns Hopkins University, Baltimore, Maryland, USA; and [4]Centre for Biomedical Imaging (CIBM), Lausanne, Switzerland

Most commonly used T_2 mapping techniques are based on 2D pulse sequences with a limited number of slices and/or low through-plane resolution. The complex 3D anatomy of cartilage surfaces of the knee motivates the need for high-resolution 3D acquisitions that provide information on the entire joint without being subject to partial volume effects. In voxels that contain multiple tissues such as cartilage and fat, these partial volume effects mix their relaxation times, which may result in T_2 measurement errors. Although 3D T_2 mapping techniques have been previously developed to improve the signal-to-noise ratio (SNR) and cartilage T_2 quantification,[7–11] there is still a need for a clinically feasible submillimetric isotropic 3D T_2 mapping technique that would allow 1) reformats in an arbitrary plane, 2) minimization of partial volume effects, 3) higher SNR per unit time compared to multiple 2D acquisitions, and 4) higher precision in T_2 relaxation time quantification.

We therefore aimed to 1) implement a high-resolution isotropic 3D T_2 mapping technique that uses sequential T_2-prepared segmented gradient-recalled echo (Iso3DGRE) images for knee cartilage evaluation and 2) to validate it both in vitro and in vivo in healthy volunteers and patients with knee OA.

Materials and Methods

Numerical Simulations

Numerical simulations of the Bloch equations[12] were performed using MatLab (MathWorks, Natick, MA) to find the optimal pulse sequence parameters (number of excitations per segment [N_{ex}] and radiofrequency (RF) excitation angle) that allowed for the maximum signal per unit time, while keeping the total scan duration as short as possible. Simulation parameters included relaxation times T_2 = 36.9 msec and T_1 = 1240 msec (similar to those of healthy cartilage),[13] a segmented *k*-space GRE acquisition with a centric readout order,[14] a repetition time (TR) of 5.2 msec, an echo time (TE) of 2.1 msec, and incremental T_2 preparation (T_2prep) durations (TE_{T2prep}) of 0/23/38/53 msec for variable T_2 weighting.[15,16] One dummy segment was simulated before the beginning of data acquisition in order to ensure a steady-state condition.

Acquisition Protocol and T_2 Fitting

We performed all MR experiments on a 3T clinical scanner (Magnetom Prisma, Siemens, Erlangen, Germany). A transmit/receive (Tx/Rx) 15-channel knee coil (Quality Electrodynamics, Mayfield, OH) was used. We implemented the Iso3DGRE pulse sequence (Fig. 1) with the parameters detailed in Table 1. An adiabatic T_2prep[16] preceded the imaging part of the sequence. The minimum duration of the T_2prep module determined the second TE_{T2prep} (ie, 23 msec). The excitation RF pulse was a 300-μs sinc pulse with a bandwidth of 20.3 kHz. A recovery time is used at the end of the acquisition to allow for longitudinal magnetization recovery and to decrease the specific absorption rate (SAR) load. The four input images were coregistered using 3D rigid registration[17,18] to account for subject motion during the acquisition. We performed pixel-wise T_2-mapping using the least-squares method in MatLab. The two-parameter fitting model used in this study is given by:

$$S(TE_{T2prep}) = S_0 \cdot \left[e^{\frac{-TE_{T2prep}}{T_2}} + \frac{\delta}{T_2} \right] \quad (1)$$

where S_0 is the initial signal when TE_{T2prep} = 0 msec and δ is an empirical offset.[19] Given the long segmental acquisition time, the empirically determined T_2-fitting offset was added in order to correct for T_1 recovery.[15,20] We made this empirical offset sensitive to the T_2 relaxation time for more accurate fitting.

Phantom Studies

We performed phantom studies to validate the results obtained from the simulations, to determine the fit offset δ, and then to test the in vitro accuracy in T_2 determination of the pulse sequence. Five phantoms were designed to approximate cartilage properties. They consisted of 0.73 μM $NiCl_2$ and varying concentration of agar (3–5% w/v), and T_2 maps were generated with the commercially available, clinical routine 2D multislice multiecho spin echo (MSME) pulse sequence and the Iso3DGRE. In Iso3DGRE the TE_{T2prep} series was similar to the TE series of MSME. Since echoes 2–6 in the MSME pulse sequence contain a signal component from the stimulated echo, the T_2 map was reconstructed by excluding the first echo.[21] We used a 2D spin-echo (SE) sequence as a T_2 reference standard, while we used an inversion-recovery spin-echo (IRSE) sequence to assure that the phantom T_1 values were similar to those of human knee cartilage. A summary of the pulse sequence parameters is reported in Table 1.

We empirically chose the T_2-fitting offset such that the intercept value in the linear regression between the reference standard SE and the Iso3DGRE phantom T_2 values was minimized. The optimal RF excitation angle of the Iso3DGRE T_2 mapping pulse sequence was experimentally verified by imaging one of the agar phantoms (4% agar) with an RF excitation angle that was varied from 5–30°.

We approximated the relative SNR as the ratio between the signal in a region of interest (ROI) drawn in the phantom and the standard deviation of the noise in an ROI drawn well outside the phantom. In order to compare these experimental results to the numerical simulations, we normalized the maximal simulated signal to the maximal experimental relative SNR.

Healthy Volunteers

The Institutional Review Board (IRB) approved this cross-sectional study and we obtained written informed consent before each examination. The study group consisted of 13 healthy adult volunteers (eight men, body mass index [BMI] 25.5 ± 3.0 kg/m^2, average age 33.2 years, range 27–39 years; five women, BMI 21.1 ± 2.2 kg/m^2, average age 28 years, range 25–33 years). We selected all volunteers among a group of individuals who showed interest in participating in MRI research (i.e., a convenience sample) and did not have any history of knee trauma or surgery, pain, or swelling. Minimal variation in cartilage loading before each scan was ensured.

We acquired an Iso3DGRE knee T_2 map in all subjects with the readout in the head–foot direction. The image with

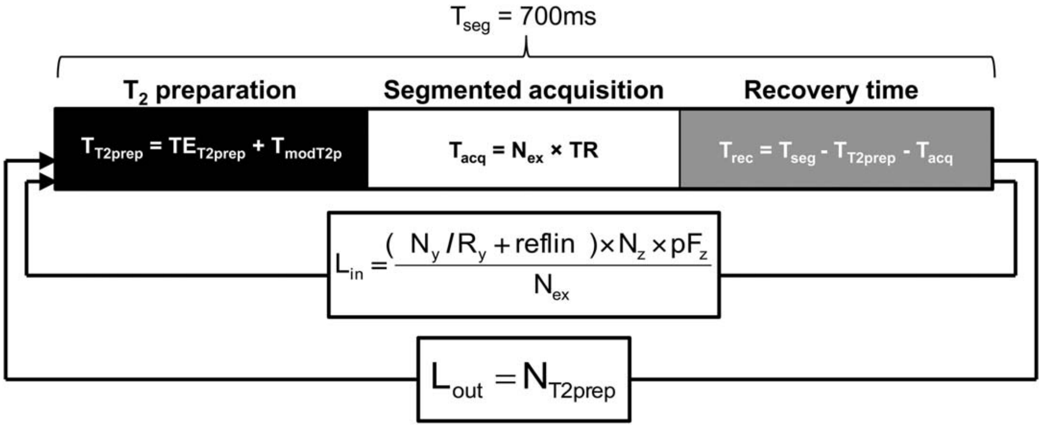

FIGURE 1: Schematic representation of the Iso3DGRE pulse sequence. The segment that is repeated in the inner loop to create one 3D image includes the T_2 preparation module (in black), the segmented acquisition (in white), and the recovery time (in gray). The inner loop is repeated L_{in} times. T_{T2prep} is the total amount of time requested for the T_2 preparation module and includes the echo time TE_{T2prep} as well as the true module duration T_{modT2p} for playing out the other halves of the RF pulses and the spoiler gradient. T_{acq} indicates the total acquisition time per segment and is given by the repetition time (TR) multiplied with the number of excitations per segment N_{ex}. A recovery time (T_{rec}) is used at the end of the acquisition to allow for longitudinal magnetization recovery and to decrease the specific absorption rate (SAR) load. T_{rec} is calculated by subtracting T_{T2prep} and T_{acq} from the total segmented acquisition time (T_{seg}). The outer loop is repeated L_{out} times, which corresponds to the number of different T_2 preparation times N_{T2prep}. At the end of each inner loop, a segment of a 3D *k*-space with a specific T_2 weighting will have been acquired. At the end of each outer loop, a 3D dataset with different T_2 weighting will have been acquired. N_y and N_z correspond to the numbers of phase-encoding steps in the y and z directions, while pFz indicates the partial Fourier reconstruction factor in the z direction. R_y is the GRAPPA acceleration factor that is applied in the y direction with reflin reference lines.

TE_{T2prep} = 23 msec was chosen for segmentation. ROIs were manually drawn (MatLab) by a research assistant (R.C., with 3 years of experience) under the supervision of a musculoskeletal radiologist (P.O., with 8 years of experience). We chose 15 continuous slices such that the central regions of the lateral and medial condyles were covered. The femoral and the tibial cartilage were segmented on these slices, after which eight cartilage compartments were defined on the sagittal plane (femoral lateral anterior, femoral lateral central, femoral lateral posterior, tibial lateral, femoral medial anterior, femoral medial central, femoral medial posterior, and tibial medial). We used the anterior and posterior margins of, respectively, the anterior and posterior menisci to distinguish between the central and the anterior/posterior femoral compartment. Next, the average T_2 value was calculated within each resulting ROI.

We also acquired an MSME T_2 map (described above). We analyzed three slices in the central region of the lateral and medial condyles that covered the same volume analyzed for the Iso3DGRE T_2 mapping, where the image of the first echo was used for segmentation. Similar to the Iso3DGRE technique, the femoral and the tibial cartilage were segmented and eight cartilage compartments were defined.

To test the repeatability in T_2 values determination, the Iso3DGRE knee T_2 map of seven healthy volunteers (four men, BMI 26.2 ± 3.5 kg/m^2, average age 33.0 years, range 27–38 years; three women, BMI 22.1 ± 2.4 kg/m^2, average age 28.7 years, range 25–33 years) was reacquired 8 weeks after the first scan.

We performed relative SNR measurements in the lateral and medial femoral cartilage (anterior, central, and posterior) layers for both T_2 map techniques. In particular, the longest TE_{T2prep} (ie, 53 msec) Iso3DGRE image and the longest TE (ie, 78 msec) MSME image were used.

Patients With Knee OA

The IRB approved this cross-sectional study and we obtained written informed consent before each examination. The study group consisted of five consecutive (i.e., selection bias did not affect the decision of which subjects to include) adult patients (one man, BMI 28.1 kg/m^2, age 83 years; four women, BMI 25.9 ± 3.9 kg/m^2, average age 67.8 years, range 61–75 years) who were treated in our institution for knee OA. We included patients based on the analysis of postero-anterior weight-bearing radiographs, read by a musculoskeletal radiologist (P.O., with 8 years of experience). Each femorotibial compartment was graded separately using the Kellgren–Lawrence criteria[22,23]: grade 1 = doubtful OA: doubtful narrowing of joint space and possible osteophytic lipping; grade 2 = minimal OA: presence of definite osteophytes and possible joint space narrowing; grade 3 = moderate OA: moderate multiple osteophytes, definite narrowing of joint space, some sclerosis and possible deformity of bone ends; grade 4 = severe OA: presence of large osteophytes, marked narrowing of joint space, severe sclerosis and definite deformity of bone ends. We included patients with severe medial femorotibial OA (grade 4) and early lateral femorotibial OA (grade 1 [n = 1] or 2 [n = 4]). The OA grade on the patellofemoral compartment was not taken into account. Patients with a history or imaging signs of previous knee surgery or traumatic ligamentous injury, rheumatologic or crystal arthropathy of the knee, and patients with contraindications to MRI were excluded. We acquired the Iso3DGRE and MSME knee T_2 maps in all subjects with the same protocol as in the volunteer studies. ROIs were manually drawn on all cartilage surfaces with remaining cartilage and slices of interest were segmented as reported for the healthy volunteer studies.

We performed relative SNR measurements as in the volunteer studies.

TABLE 1. Pulse Sequence Parameters Used for the Parametric Mapping Techniques

Sequence parameters	Iso3DGRE	2D MSME	2D SE	2D IRSE
Slices (–)	144	36	1	1
Slice spacing (mm)	—	0.3	—	—
Repetition time (msec)	5.2	1630	7000	7000
Echo times (msec)	2.1	13, 26, 39, 52, 65, 78	6.8, 15, 30, 60, 120, 250, 400	6.8
T_2 preparation durations (msec)	0, 23, 38, 53	—	—	—
Inversion times (msec)	—	—	—	23, 50, 100, 250, 500, 1000, 2000, 4000
Receiver bandwidth (Hz/px)	301	208	300	300
Phase partial Fourier (–)	—	5/8	—	—
Slice partial Fourier (–)	3/4	—	—	—
Matrix size (–)	272 × 280 ×144	320 × 224	192 × 92	192 × 92
Acquired voxel volume (mm^3)	0.63 × 0.63 × 0.63	0.52 × 0.73 x 3	1.3 × 1.3 × 6	1.3 × 1.3 × 6
GRAPPA factor* (–)	2×	2×	—	—
Scan time (min)	10.1	7.2	75	85

Iso3DGRE isotropic three-dimensional T_2-prepared segmented gradient-recalled echo; 2D MSME two-dimensional multislice multiecho; 2D SE two-dimensional spin- echo; 2D IRSE two-dimensional inversion-recovery spin-echo; GRAPPA generalized autocalibrating partially parallel acquisitions.
*Indicates GRAPPA acceleration applied in the in-plane phase encoding direction (y).

Statistical Analysis

We conducted statistical analyses with GraphPad Prism 6.0 (GraphPad Software, La Jolla, CA), MatLab, and computing environment R (R Development Core Team, Vienna, Austria). The correlation and accuracy of both T_2 mapping techniques and the reference standard SE were assessed with linear regression and Bland–Altman analysis.[24] For each compartment, we analyzed the distribution of the T_2 values for each subject and for the femur and the tibia separately. We excluded extreme outlier T_2 values that were beyond cartilage T_2 relaxation time physiological range from the analysis, since they were most likely the result of misregistration[25] or partial volume effect; a T_2 value was considered to be an extreme outlier if its distance to the interquartile interval of the ROI exceeded three times the length of this interval. Next, we calculated the mean T_2 value and standard deviation of each compartment for both the patient and volunteer groups. A two-tailed Student's *t*-test was performed together with a Bland–Altman analysis in order to evaluate the difference in T_2 values between patient and volunteers and between the Iso3DGRE and the MSME techniques, respectively. For in vitro and in vivo studies, we calculated the inverse of the precision of each technique as the ratio of the standard deviation and the average T_2 value within the ROIs (i.e., relative standard deviation). Finally, the repeatability of the T_2 mapping was determined using the coefficient of variation (CoV), the intraclass correlation coefficient (ICC),[26] and the Bland–Altman analysis. Statistical significance was defined as $P < 0.05$.

Results

Numerical Simulations

The optimized sequence parameters included 100 excitations per segment (Fig. 2a) and RF excitation angle = 15° (Fig. 2b). The minimum segmental acquisition time (T_{seg}) was determined at the scanner due to SAR limits and was 700 msec.

Phantom Studies

The T_2 relaxation times ranged from 25.96 ± 1.03 msec to 49.36 ± 1.59 msec. The IRSE reference T_1 relaxation time of all five phantoms was 1340.4 ± 15.0 msec. In the phantom studies (Fig. 3a–c), Iso3DGRE T_2 mapping slightly underestimated the SE T_2 values (linear fit slope 0.9 ± 0.05) when the fit offset δ was set to 3, while the MSME technique slightly overestimated them (linear fit slope 1.05 ± 0.07). Given the negligible linear fit intercept (0.2 ± 1.7 msec), the relationship between the T_2 values obtained with the SE and the Iso3DGRE technique was directly proportional, as opposed to that between the SE and MSME T_2 values (linear fit intercept 3.5 ± 2.6 msec). A high goodness of fit of the linear regression between the SE and the Iso3DGRE T_2 maps was observed (R^2 = 0.99), while a similarly

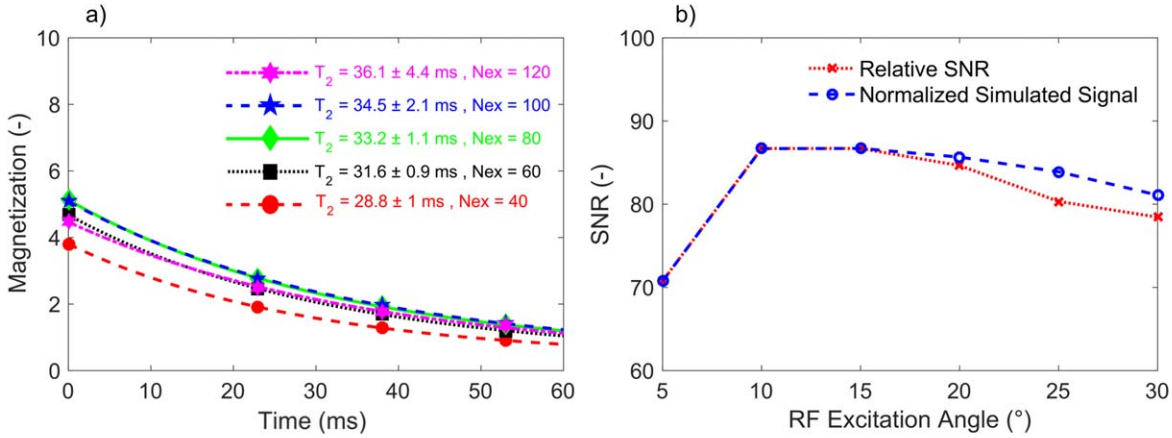

FIGURE 2: Protocol optimization through Bloch equation simulations. (a) The magnetization as a function of time (TE_{T2prep}) for different number of excitations per segment (N_{ex}). The minimum segmental acquisition time was 700 msec due to specific absorption rate (SAR) constraints and the optimal N_{ex} that allowed maximizing the simulated magnetization was 100. (b) The relative signal-to-noise ratio (SNR) in the phantom experiment and the normalized simulated signal as a function of the radiofrequency (RF) excitation angle for TE_{T2prep} = 23 msec show a very similar curve shape, and resulted in an optimal RF excitation angle of 15°.

high goodness of fit (R^2 = 0.98) was found between the SE and MSME T_2 maps.

Averaged over all agar phantoms, the relative standard deviations were 2.6 ± 0.4% (Iso3DGRE) and 3.1 ± 1.0% (MSME, P = 0.1).

The Bland–Altman analysis resulted in a slightly smaller bias for the Iso3DGRE (–3.7 msec, P = 0.002, Fig. 3d) than for the MSME technique (5.4 msec, P < 0.001, Fig. 3e). Compared to the SE T_2 values, the Iso3DGRE T_2 values better agreed than those obtained with the MSME technique for smaller T_2 values. A minor trend of underestimation was found in Iso3DGRE T_2 values, as opposed to the overestimation trend produced by the MSME technique. The limits of agreement were the same for both techniques (±2.3 msec, Fig. 3d,e). The optimal RF excitation angle (15°) was experimentally determined and was in accordance with the simulated one for all TE_{T2prep} (Fig. 2b).

Healthy Volunteers

In all the eight compartments and in accordance with what was observed in the phantom study, the Iso3DGRE T_2 values were significantly lower than those determined with the MSME technique (P < 0.001 for all comparisons, Fig. 4a,b, Table 2) and allowed for multiplanar reformatting (Fig. 5). The Bland–Altman analysis resulted in a bias of –10.2 msec (P < 0.001) and limits of agreement of ±5.6 msec (Fig. 4c).

Averaged over all volunteers and compartments, the relative standard deviations were 26.8 ± 8.2% (Iso3DGRE) and 26.6 ± 8.6% (MSME, P = 0.81).

The CoV varied from 1.1% for the femoral lateral central compartment to 9.1% for the tibial medial compartment, while the ICC varied from 0.89 for the femoral lateral central compartment to 0.43 for the femoral lateral anterior compartment (Table 3). The Bland–Altman analysis resulted in a bias of –0.70 msec (P = 0.42) and limits of agreement of ±4.5 msec.

Averaged over all cartilage compartments and over all volunteers, the relative SNR was 13.7 ± 0.2 for Iso3DGRE and 48.7 ± 4.4 for MSME.

Patients With Knee OA

In the OA knees, the articular cartilage was missing in the tibial medial, femoral medial anterior, and femoral medial central compartments (these compartments were not included in the analysis). In all the remaining compartments we found a significant difference (P < 0.03 for all comparisons) between the T_2 values obtained with the Iso3DGRE technique and the values obtained with the MSME T_2 mapping technique, similar to what we observed in the phantom and volunteer studies (Table 2). The Bland–Altman analysis resulted in a bias of –15.6 msec (P < 0.003) and limits of agreement of ± 10.2 msec (Fig. 4d). Moreover, in each compartment the average T_2 values obtained with both the Iso3DGRE and the MSME sequences were higher in OA compared to healthy knees (P < 0.03 and P < 0.02, respectively, for all comparisons), except for the femoral lateral central compartment (P = 0.38 and P = 0.82, respectively). Averaged over all patients and compartments, the relative standard deviations were significantly lower for the Iso3DGRE compared to the MSME sequence (23.0 ± 8.1% vs. 28.1 ± 8.6%, respectively, P = 0.01).

Averaged over all cartilage compartments and over all patients, the relative SNR was 15.0 ± 1.1 for Iso3DGRE and 69.0 ± 0.2 for MSME.

Discussion

In this study we developed and optimized a new isotropic 3D T_2 mapping technique of knee cartilage. We validated our sequence through phantom studies that demonstrated a good correlation between T_2 values obtained with the

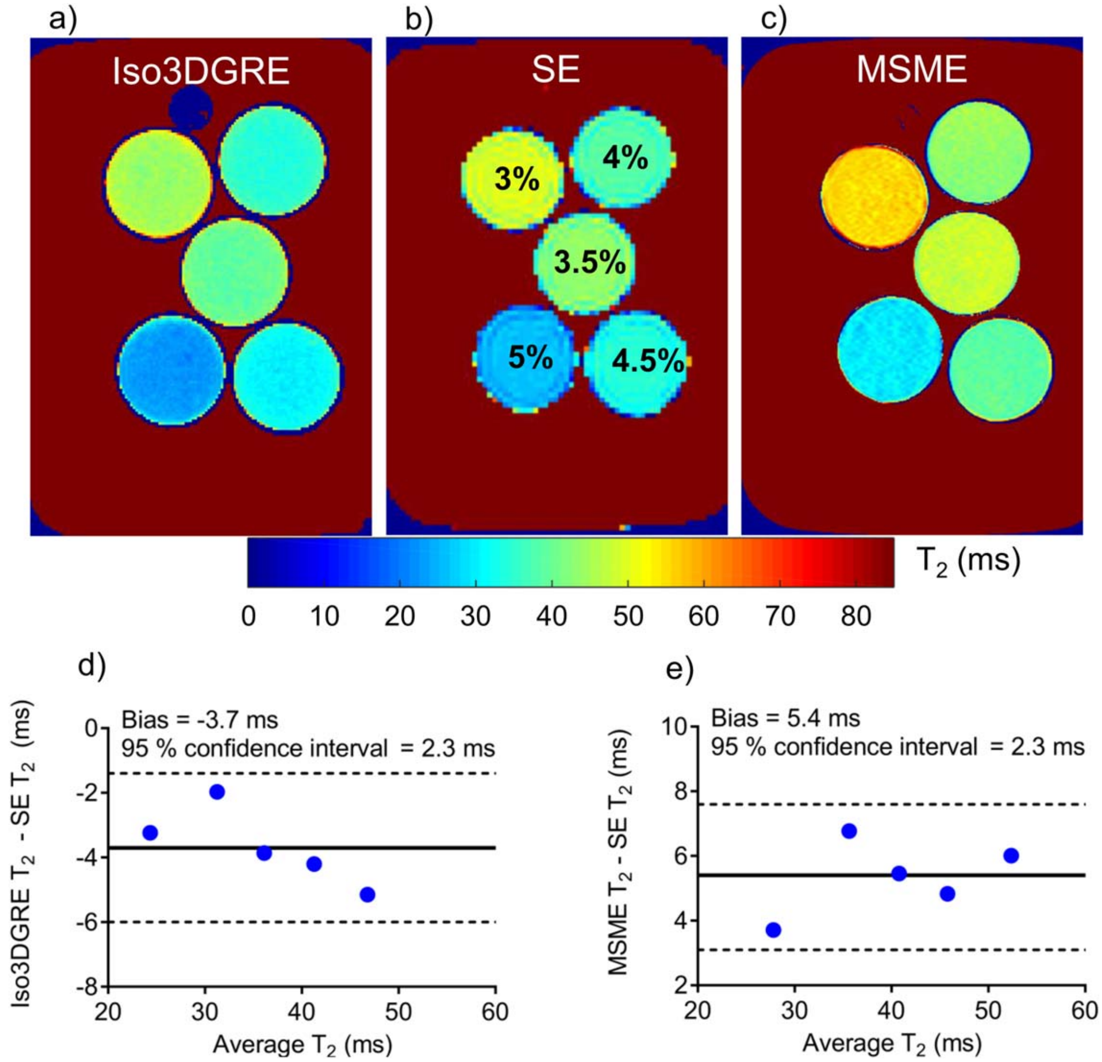

FIGURE 3: In vitro comparison between three T_2 mapping techniques. (a) An Iso3DGRE, (b) an SE, and (c) an MSME T_2 map of five phantoms with similar T_1 relaxation times and a range of T_2 relaxation times as a function of agar concentration (3–5% weight/volume) that approximate those of cartilage. The percentage of agar is indicated in the middle map. SE T_2 values range from 26.0 ± 1.0 msec to 49.4 ± 1.6 msec as a function of the agar concentration. Neither Iso3DGRE (difference up to –12%) nor MSME (difference up to 20%) agreed directly with SE for any phantom. (d) The Iso3DGRE T_2 mapping technique resulted in a bias of –3.7 msec (P = 0.002) and limits of agreement of ± 2.3 msec. (e) The MSME technique resulted in a bias of 5.4 msec (P < 0.001) and limits of agreement of ± 2.3 msec. The dashed lines indicate the limits of agreement. A minor trend of underestimation in Iso3DGRE T_2 values when compared to the SE-derived can be observed, as opposed to the overestimation trend produced by the MSME technique.

proposed technique and the SE reference standard. In vitro, the Bland–Altman analysis resulted in a smaller bias for the Iso3DGRE than for the MSME technique, indicating that the Iso3DGRE technique might have slightly higher accuracy in T_2 determination, while the precision was the same for both techniques. However, the T_2 values in the range of interest were slightly underestimated for Iso3DGRE, while for MSME the T_2 values were overestimated, as established in several prior studies.[27,28] Given the negligible intercept value that resulted from the linear regression between the SE reference standard and the Iso3DGRE-derived T_2 values (0.2 msec), this underestimation can potentially be corrected simply by using a scaling factor, if desired. In contrast, the standard MSME T_2 mapping technique resulted in overestimated T_2 values with equivalent (healthy volunteers) or even higher standard deviation (patients with OA) compared to those obtained with the proposed technique. An empirical offset might also be used to improve the accuracy of the MSME pulse sequence, but this was beyond the goal of the present study. The Iso3DGRE technique is thus characterized by higher precision in vivo, even if the acquired voxel volume was 4.5 times smaller than that of MSME. The difference in precision performance between the in vitro and in vivo studies might be caused by the lower motion sensitivity of Iso3DGRE due to the sequential acquisition and the source image coregistration. Conversely, the intrinsic acquisition strategy of the MSME pulse sequence removes the benefit of any potential image coregistration: since each echo train acquires a line of each image, all images are subject to all motion that occurs, and the

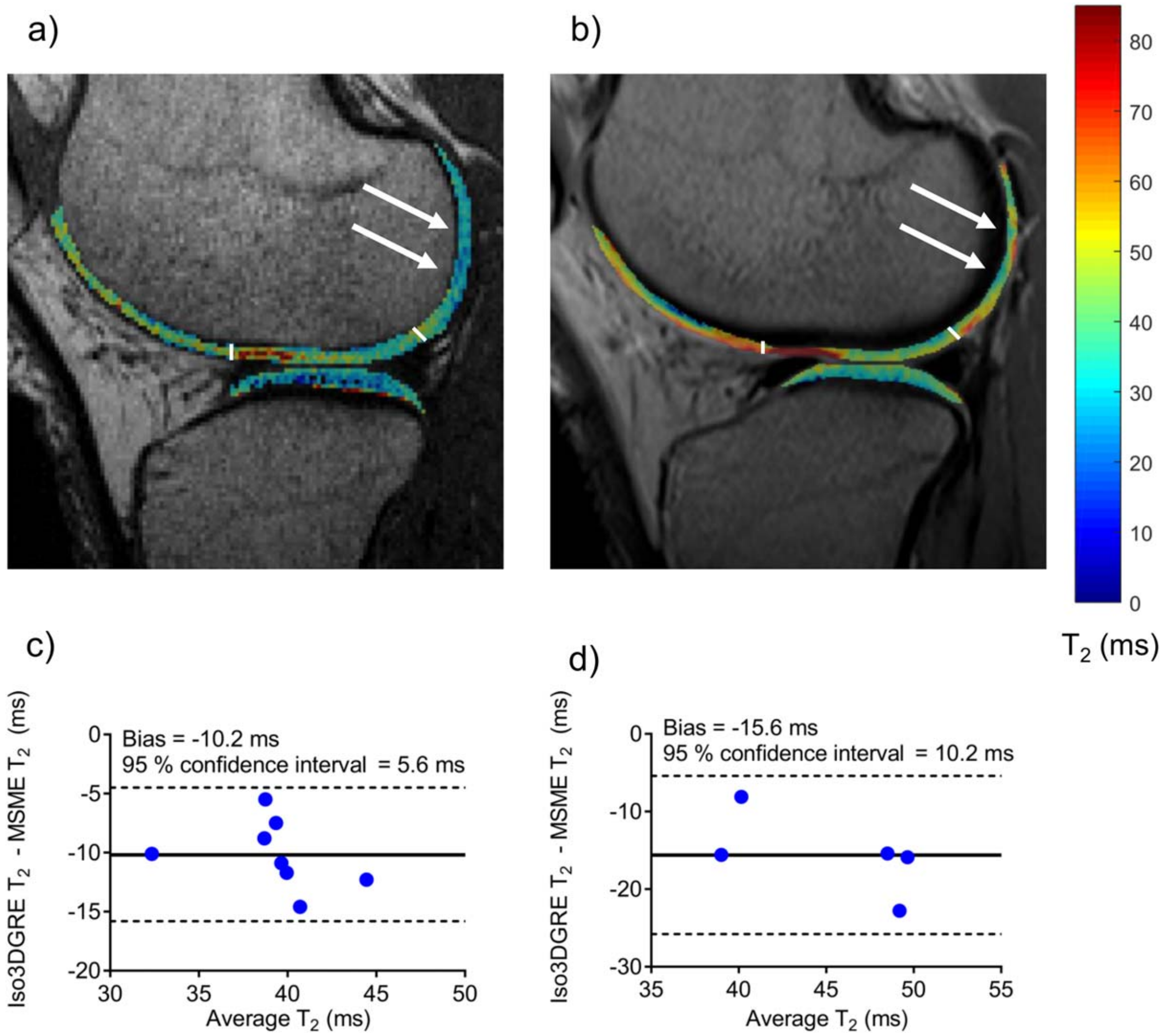

FIGURE 4: Representative segmented T_2 maps and in vivo comparison between two T_2 mapping techniques. (a) Iso3DGRE T_2 map overlaid on related morphological image (TE_{T2prep} = 23 msec) and (b) MSME T_2 map overlaid on related morphological image (TE = 13 msec). Femoral and tibial cartilage in both lateral and medial regions were manually segmented and then divided into four additional compartments (white divider lines). The Iso3DGRE T_2 map is visually characterized by less pronounced chemical shift artifacts compared to the MSME T_2 map (white arrows). (c) A Bland–Altman analysis of the Iso3DGRE versus the MSME in the volunteer studies resulted in a bias of –10.2 msec ($P < 0.001$) and limits of agreement of ± 5.6 msec. (d) Similarly, the Bland–Altman analysis of the patient studies resulted in a bias of –15.6 msec ($P < 0.003$) and limits of agreement of ± 10.2 msec. In both analyses, the Iso3DGRE T_2 values were significantly lower than those determined with the MSME technique.

images do not have different motion states that can be corrected with respect to one another.

We furthermore validated the technique in both healthy volunteers and OA patients. In particular, we measured T_2 values of preserved areas of cartilage in severely medial femorotibial osteoarthritic knees. These areas included the lateral femorotibial and the posterior medial femoral compartments. Previous studies have shown that: 1) the apparently preserved cartilage in unicompartmental OA shows histological and mechanical signs of early OA,[29–31] and 2) the posterior aspect of the femoral compartment affected by advanced stages of OA is preserved in up to 89% of patients while presenting hypertrophy, possibly due to swelling that occurs in early OA changes.[32,33] Repeated cartilage T_2 value measurements showed a small CoV (5.6%) and both the Iso3DGRE and MSME sequences demonstrated increased T_2 values with OA in most compartments, as expected.[4,6]

The main advantage of the Iso3DGRE technique is its high-resolution isotropic acquisition, which results in a voxel size that is about 3 times smaller (0.25 mm^3 vs. 0.75 mm^3) than currently available T_2 mapping sequences,[28] and is comparable to the voxel size of routinely used 3D morphological sequences (~0.125 mm^3). Several morphological studies have shown that cartilage properties present great regional variations.[32–37] Since this variability is assessed at high resolution, there is a need to correlate morphologic and compositional/biochemical data to better understand these changes, and the lack of submillimetric isotropic resolution of the latter has been a limiting factor so far.

At 10 minutes, the acquisition time of the proposed isotropic 3D T_2 mapping technique was slightly longer than that of clinical routine T_2 mapping protocols, which usually take between 4 and 9 minutes.[7,8,11] However, this increased

TABLE 2. Average Cartilage T_2 Values in Healthy Volunteers and Patients With Advanced Knee OA

	FLA	FLC	FLP	TL	FMA	FMC	FMP	TM
Iso3DGRE T_2 values (msec)								
Healthy volunteers	33.4 ± 3.4*	34.2 ± 4.1	34.1 ± 2.4*	27.3 ± 3.2*	38.3 ± 4.5	36.0 ± 4.7	34.3 ± 2.5*	35.6 ± 4.2
Advanced OA patients	37.8 ± 2.7*	36.1 ± 3.7	41.7 ± 1.2*	31.2 ± 2.5*	—	—	40.8 ± 3.3*	—
MSME T_2 values (msec)								
Healthy volunteers	48.0 ± 4.3*	45.1 ± 8.7	45.8 ± 4.2*	37.4 ± 3.6*	50.6 ± 8.2	41.5 ± 4.4	43.1 ± 1.7*	43.1 ± 5.7
Advanced OA patients	60.6 ± 12.4*	44.2 ± 2.4	57.6 ± 4.9*	46.8 ± 11.0*	—	—	56.2 ± 11.0*	—

FLA femoral lateral anterior; FLC femoral lateral central; FLP femoral lateral posterior; TL tibial lateral; FMA femoral medial anterior; FMC femoral medial central; FMP femoral medial posterior; TM tibial medial.
*Indicates significant difference in values between groups of subjects, $P < 0.03$.

acquisition time can be justified with the possibility of multiplanar reformatting: the isotropic data allows for the evaluation of the distribution of cartilage T_2 values in any reformatted plane, and thus the complete coverage of the articular surface. This might represent an improvement in knee cartilage imaging, since multiple time-consuming 2D acquisitions in different planes are no longer necessary, partial volume effects in the slice direction are avoided, and T_2 precision and accuracy are improved. Multiple 3D T_2 mapping techniques for knee cartilage quantification have been developed, including double echo steady state (DESS),[7,8] triple echo steady state (TESS),[9] and spoiled gradient-echo (SPGR).[10,11] However, these studies mainly aimed at using a 3D approach to improve SNR and were limited by their anisotropic resolution, as a consequence of the trade-off between SNR and acquisition time. The average relative cartilage SNR for the in vivo studies was 15 in the longest $TE_{T2\text{-}prep}$ image of the Iso3DGRE technique, and 59 in the longest TE image for MSME. This relative SNR represents just an approximation, since the setup made use of a phased array coil, and GRAPPA was enabled. As reported by Sandino et al,[38] an SNR of 15 in a 15-element RF coil should lead to a signal overestimation of ~5%, which might lead to a negligible T_2 relaxation time overestimation of 3%.

The present study has several limitations. First, the number of analyzed subjects was relatively small. This might be responsible for the absence of a significant difference, although expected,[6] in the femoral lateral central cartilage Iso3DGRE T_2 values between healthy subjects and patients with OA. Second, in order to keep the total acquisition time as short as possible, we did not use any fat signal suppression technique. Such a technique would allow for increased contrast at the subchondral bone–cartilage interface and suppression of chemical shift artifacts, but at the expense of longer acquisition time. However, McGibbon et al[39] have demonstrated through cartilage thickness measurements that the effect of chemical shift artifacts (both phase-cancellation and misregistration) is not substantial with gradient echo sequences. In the present study, the effect of chemical shift was indeed minimal on the Iso3DGRE maps compared to the MSME maps. Third, the magic angle effect on the T_2 map was not specifically investigated in this study. The use of T_2 values averaged over compartments allowed the minimization of its bias. Fourth, we used the coregistration to only correct for rigid motion between acquisitions. Any motion during the acquisition or any residual nonrigid motion was not taken into account. However, given the rigid structure of the cartilage layer and the physical restraints we used to minimize knee mobility, we made the hypothesis that most subject motion was small and

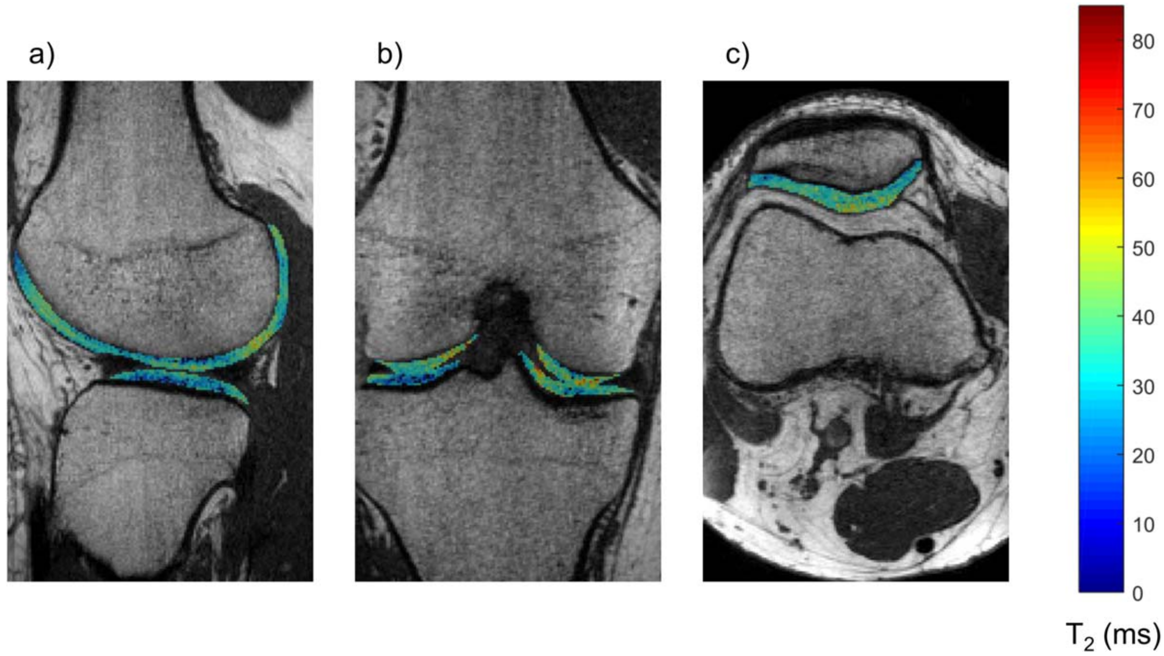

FIGURE 5: A T_2 map of a healthy volunteer acquired by Iso3DGRE overlaid on a morphological image. (a) Sagittal view of a knee for TE_{T2prep} = 23 msec. The color-coded T_2 map was overlaid. (b) Reformatted coronal and (c) axial view of the same volunteer on which the T_2 map was overlaid. All views have identical pixel sizes.

only translational. Fifth, our pulse sequence parameters were optimized separately due to the interplay between SAR limits, stimulation limits, and parameter settings. Finally, neither the magnetization transfer nor the diffusion effects on T_2 relaxation time quantification were quantified.

For future developments, by applying model-based compressed sensing,[40] it should be possible to reduce the acquisition time or to improve the spatial resolution. The regularization effect intrinsic to the compressed sensing reconstruction would most likely result in more precise T_2 relaxation times. Moreover, this potential time economy could be exploited to apply a time-consuming fat signal suppression technique (such as using spectrally selective RF pulses). Finally, the stability of the empirical offset used in this study when varying pulse sequence parameters should be investigated in a future study.

TABLE 3. Coefficient of Variation (CoV) and Intraclass Correlation Coefficient (ICC) for Repeated T_2 Value Measurements in Healthy Volunteers

Cartilage compartment	T_2 CoV (%)	ICC
Femoral lateral anterior	8.3	0.43
Femoral lateral central	1.1	0.89
Femoral lateral posterior	7.2	0.64
Tibial lateral	2.1	0.77
Femoral medial anterior	4.8	0.64
Femoral medial central	4.5	0.87
Femoral medial posterior	7.5	0.62
Tibial medial	9.1	0.49
All	5.6	—

The Bland–Altman analysis resulted in a bias of –0.70 msec (P = 0.42) and limits of agreement of ± 4.5 msec.

In conclusion, we developed, optimized, and validated a new isotropic 3D T_2 mapping technique of knee cartilage in phantoms, volunteers, and patients. This technique allows for isotropic acquisition, which is advantageous for the complex knee anatomy. Due to its reasonable acquisition time, this sequence could be used in larger cohorts of patients to provide valuable 3D quantitative data on cartilage and other structures involved in OA such as the menisci, in order to improve our understanding of the disease and test new therapeutic solutions.

Acknowledgments

Contract grant sponsor: Pierre Mercier Foundation; Contract grant sponsor: Swiss National Science Foundation; contract grant number: PZ00P3-154719 (to RBvH); Contract grant sponsor: R'Equip grant from the Swiss National Science Foundation; contract grant number: 326030_150828 (to M.S.); Contract grant sponsor: Centre d'Imagerie BioMédicale (CIBM) of the UNIL, UNIGE, HUG, CHUV, EPFL, and the Leenaards and Jeantet Foundations.
The authors thank Prof. Matthias Stuber for fruitful discussions and the MR technologists of the CHUV for their extensive help with the MR scanning.

References

1. Link TM, Neumann J, Li X. Prestructural cartilage assessment using MRI. J Magn Reson Imaging 2017;45:949–965.
2. Roemer FW, Crema MD, Trattnig S, Guermazi A. Advances in imaging of osteoarthritis and cartilage. Radiology 2011;260:332–354.
3. Guermazi A, Crema MD, Roemer FW. Compositional magnetic resonance imaging measures of cartilage—endpoints for clinical trials of disease-modifying osteoarthritis drugs? J Rheumatol 2016;43:7–11.
4. David-Vaudey E, Ghosh S, Ries M, Majumdar S. T2 relaxation time measurements in osteoarthritis. Magn Reson Imaging 2004;22:673–682.
5. Guermazi A, Roemer FW, Alizai H, et al. State of the art: MR imaging after knee cartilage repair surgery. Radiology 2015;277:23–43.
6. Dunn TC, Lu Y, Jin H, Ries MD, Majumdar S. T2 relaxation time of cartilage at MR imaging: comparison with severity of knee osteoarthritis. Radiology 2004;232:592–598.
7. Welsch GH, Scheffler K, Mamisch TC, et al. Rapid estimation of cartilage T2 based on double echo at steady state (DESS) with 3 Tesla. Magn Reson Med 2009;62:544–549.
8. Staroswiecki E, Granlund KL, Alley MT, Gold GE, Hargreaves BA. Simultaneous estimation of T(2) and apparent diffusion coefficient in human articular cartilage in vivo with a modified three-dimensional double echo steady state (DESS) sequence at 3 T. Magn Reson Med 2012;67:1086–1096.
9. Heule R, Ganter C, Bieri O. Triple echo steady-state (TESS) relaxometry. Magn Reson Med 2014;71:230–237.
10. Bolbos RI, Zuo J, Banerjee S, et al. Relationship between trabecular bone structure and articular cartilage morphology and relaxation times in early OA of the knee joint using parallel MRI at 3 T. Osteoarthritis Cartilage 2008;16:1150–1159.
11. Pai A, Li X, Majumdar S. A comparative study at 3 T of sequence dependence of T2 quantitation in the knee. Magn Reson Imaging 2008;26:1215–1220.
12. Bloch F. Nuclear induction. Phys Rev 1946;70:460–474.
13. Gold GE, Han E, Stainsby J, Wright G, Brittain J, Beaulieu C. Musculoskeletal MRI at 3.0 T: relaxation times and image contrast. AJR Am J Roentgenol 2004;183:343–351.
14. Bernstein MA, King KF, Zhou XJ. Handbook of MRI pulse sequences. Amsterdam: Elsevier; 2004.
15. van Heeswijk RB, Feliciano H, Bongard C, et al. Free-breathing 3 T magnetic resonance T2-mapping of the heart. JACC Cardiovasc Imaging 2012;5:1231–1239.
16. Nezafat R, Stuber M, Ouwerkerk R, Gharib AM, Desai MY, Pettigrew RI. B1-insensitive T2 preparation for improved coronary magnetic resonance angiography at 3 T. Magn Reson Med 2006;55:858–864.
17. Studholme C, Hill DL, Hawkes DJ. Automated 3-D registration of MR and CT images of the head. Med Image Anal 1996;1:163–175.
18. Bonanno G, Puy G, Wiaux Y, van Heeswijk RB, Piccini D, Stuber M. Self-navigation with compressed sensing for 2D translational motion correction in free-breathing coronary MRI: a feasibility study. PLoS One 2014;9:e105523.
19. van Heeswijk RB, Piccini D, Feliciano H, Hullin R, Schwitter J, Stuber M. Self-navigated isotropic three-dimensional cardiac T2 mapping. Magn Reson Med 2015;73:1549–1554.
20. Bano W, Feliciano H, Coristine AJ, Stuber M, van Heeswijk RB. On the accuracy and precision of cardiac magnetic resonance T2 mapping: A high-resolution radial study using adiabatic T2 preparation at 3 T. Magn Reson Med 2017;77:159–169.
21. Smith HE, Mosher TJ, Dardzinski BJ, et al. Spatial variation in cartilage T2 of the knee. J Magn Reson Imaging 2001;14:50–55.
22. Kellgren JH, Lawrence JS. Radiological assessment of osteo-arthrosis. Ann Rheum Dis 1957;16:494–502.
23. Schiphof D, Boers M, Bierma-Zeinstra SM. Differences in descriptions of Kellgren and Lawrence grades of knee osteoarthritis. Ann Rheum Dis 2008;67:1034–1036.
24. Bland JM, Altman DG. Statistical methods for assessing agreement between two methods of clinical measurement. Lancet 1986;1:307–310.
25. Raya JG, Dietrich O, Horng A, Weber J, Reiser MF, Glaser C. T2 measurement in articular cartilage: impact of the fitting method on accuracy and precision at low SNR. Magn Reson Med 2010;63:181–193.
26. Shrout PE, Fleiss JL. Intraclass correlations: uses in assessing rater reliability. Psychol Bull 1979;86:420–428.
27. Maier CF, Tan SG, Hariharan H, Potter HG. T2 quantitation of articular cartilage at 1.5 T. J Magn Reson Imaging 2003;17:358–364.
28. Juras V, Bohndorf K, Heule R, et al. A comparison of multi-echo spin-echo and triple-echo steady-state T2 mapping for in vivo evaluation of articular cartilage. Eur Radiol 2016;26:1905–1912.
29. Obeid EM, Adams MA, Newman JH. Mechanical properties of articular cartilage in knees with unicompartmental osteoarthritis. J Bone Joint Surg Br 1994;76:315–319.
30. Bert JM, Leverone J. Histologic appearance of "pristine" articular cartilage in knees with unicompartmental osteoarthritis. J Knee Surg 2007;20:15–19.
31. Moen TC, Laskin W, Puri L. The lateral compartment in knees with isolated medial and patellofemoral osteoarthritis: a histologic analysis of articular cartilage. J Arthroplasty 2011;26:783–787.
32. Omoumi P, Michoux N, Roemer FW, Thienpont E, Vande Berg BC. Cartilage thickness at the posterior medial femoral condyle is increased in femorotibial knee osteoarthritis: a cross-sectional CT arthrography study (Part 2). Osteoarthritis Cartilage 2015;23:224–231.
33. Omoumi P, Michoux N, Thienpont E, Roemer FW, Vande Berg BC. Anatomical distribution of areas of preserved cartilage in advanced femorotibial osteoarthritis using CT arthrography (Part 1). Osteoarthritis Cartilage 2015;23:83–87.
34. Favre J, Erhart-Hledik JC, Blazek K, Fasel B, Gold GE, Andriacchi TP. Anatomically–standardized maps reveal distinct patterns of cartilage thickness with increasing severity of medial compartment knee osteoarthritis. J Orthop Res 2017 [Epub ahead of print].
35. Shiomi T, Nishii T, Nakata K, et al. Three-dimensional topographical variation of femoral cartilage T2 in healthy volunteer knees. Skeletal Radiol 2013;42:363–370.
36. Kaneko Y, Nozaki T, Yu H, et al. Normal T2 map profile of the entire femoral cartilage using an angle/layer-dependent approach. J Magn Reson Imaging 2015;42:1507–1516.
37. Wirth W, Maschek S, Eckstein F. Sex- and age-dependence of region- and layer-specific knee cartilage composition (spin-spin-relaxation time) in healthy reference subjects. Ann Anat 2017;210:1–8.
38. Sandino CM, Kellman P, Arai AE, Hansen MS, Xue H. Myocardial T2* mapping: influence of noise on accuracy and precision. J Cardiovasc Magn Reson 2015;17:7.
39. McGibbon CA, Bencardino J, Palmer WE. Subchondral bone and cartilage thickness from MRI: effects of chemical-shift artifact. MAGMA 2003;16:1–9.
40. Huang C, Graff CG, Clarkson EW, Bilgin A, Altbach MI. T2 mapping from highly undersampled data by reconstruction of principal component coefficient maps using compressed sensing. Magn Reson Med 2012;67:1355–1366.